nature physics

LETTERS

PUBLISHED ONLINE: 5 OCTOBER 2015 | DOI: 10.1038/NPHYS3491

# Observation of a persistent non-equilibrium state in cold atoms

D. S. Lobser[1,2], A. E. S. Barentine[1,2], E. A. Cornell[1,2] and H. J. Lewandowski[1,2]*

**Boltzmann noticed that his transport equation predicts special cases in which gases never reach thermal equilibrium. One example is the monopole breathe mode of atoms confined in a perfectly isotropic three-dimensional (3D) harmonic potential[1]. Such a complete absence of damping had not been observed in nature, and this anomaly weakened Boltzmann's then-controversial claim to have established a microscopic, atomistic basis for thermodynamics. Only recently has non-damping of a monopole mode in lower-dimensional systems been reported in cold-atom experiments performed in highly elongated trap geometries[2,3]. The difficulty in generating a sufficiently spherical harmonic confinement for cold atoms has so far prevented the observation of Boltzmann's fully 3D, isotropic case. Here, thanks to a new magnetic trap[4] capable of producing near-spherical harmonic confinement for cold atoms, we report a long-delayed vindication for Boltzmann: the observation of a 3D monopole mode for which the collisional contribution to damping vanishes.**

The Boltzmann equation determines how the phase-space distribution of a gas, $f(\mathbf{r},\mathbf{v},t)$, evolves as a function of time, $t$, with binary collisions between particles with mass, $m$, in the presence of an external force, $\mathbf{F}$

$$\frac{\mathrm{d}f}{\mathrm{d}t}=\frac{\partial f}{\partial t}+\mathbf{v}\cdot\nabla_{\mathbf{r}}f+\frac{\mathbf{F}}{m}\cdot\nabla_{\mathbf{v}}f=I_{\mathrm{coll}}[f] \tag{1}$$

The collision integral, $I_{\mathrm{coll}}$, describes how populations at the same location, $\mathbf{r}$, but differing velocities, $\mathbf{v}$, redistribute to two new velocities, $\mathbf{v}'$. These local, pairwise collisions conserve momentum and energy. For the explicit form of the integral, see refs 5,6.

The collision integral vanishes whenever the product of two single-particle distributions is identical directly before and after a collision, in other words, when

$$f(\mathbf{v}_1)f(\mathbf{v}_2)=f(\mathbf{v}_1')f(\mathbf{v}_2') \tag{2}$$

This equality typically implies that the phase-space distribution is time invariant and the gas has reached equilibrium. However, when energy, momentum and total atom number are conserved, equation (2) is generically satisfied by distributions of the form

$$f(\mathbf{r},\mathbf{v},t)\propto A(\mathbf{r})\mathrm{e}^{-\frac{|m\mathbf{v}-\eta(\mathbf{r},t)|^2}{2mk_{\mathrm{B}}T(t)}} \tag{3}$$

where $A(\mathbf{r})$ contains information about the external confining potential, $k_{\mathrm{B}}$ is the Boltzmann constant, the temperature $T(t)$ is time dependent, and $\eta(\mathbf{r},t)$ is an arbitrary function of space and time. Although these distributions, known as 'local equilibrium distributions', always cause the collision integral to vanish, they in general do not satisfy equation (1) (refs 5–8). By constraining the local equilibrium distribution so that $\eta(\mathbf{r},t)=0$ and $\mathrm{d}T/\mathrm{d}t=0$, the distribution becomes a valid solution of equation (1) and is known as the Maxwell–Boltzmann distribution:

$$f(\mathbf{r},\mathbf{v})\propto A(\mathbf{r})\mathrm{e}^{-\frac{mv^2}{2k_{\mathrm{B}}T}}$$

But certain potentials exist where equation (1) is satisfied by non-equilibrium distributions, in which case the time dependence in equation (3) remains[7,8]. One of these cases is the three-dimensional (3D) isotropic harmonic potential with a solution corresponding to a spherically symmetric 'monopole mode', where temperature and cloud size oscillate, with opposite phase, in time[8–10]. Because the temperature is oscillating in the absence of heat conduction, it is convenient to call the temperature in equation (3) a 'kinetic temperature', $T_{\mathrm{k}}(t)$, and define a 'spatial temperature', $T_{\mathrm{s}}(t)$, which determines the variation in cloud size. The average temperature $(T_{\mathrm{k}}(t)+T_{\mathrm{s}}(t))/2$ is constant; the breathing dynamics are analogous to the oscillatory exchange between kinetic and potential energy that occurs in simple harmonic motion. Although the structure of equation (1) implies a quasicontinuous distribution $f$, and thus very large atom number $N$, we show in Methods that the result of vanishing damping is preserved as $N$ increases from 1 to 2, and onto an arbitrary meso- or macroscopic number.

This strange absence of damping holds for the monopole mode, but not necessarily for other collective modes. For the quadrupole mode, a mode in which the radial and axial widths oscillate 180° out of phase, cross-dimensional coupling from collisions causes damping. In the limit of an interatomic collision rate, $\gamma_{\mathrm{coll}}$, that is much smaller than the trap frequency, the quadrupole mode in an isotropic harmonic potential is predicted to damp at a rate[9]

$$\Gamma_{\mathrm{Q}}\simeq 0.2\,\gamma_{\mathrm{coll}} \tag{4}$$

We measure quadrupole damping rates as a baseline for comparison with measured monopole damping rates.

The experiment is performed with $^{87}$Rb atoms evaporatively cooled in a time-averaged orbiting potential[11,12] magnetic trap with harmonic confinement at frequency $\omega=2\pi(9.03(2)\,\mathrm{Hz})$, equipped with additional magnetic coils that permit the six distinct parameters of a 3D quadratic potential to be adjusted independently[4]. (See Supplementary Information for more details.) We measure dipole sloshing motion of atoms in the trap to determine $\hat{i}$, $\hat{j}$, $\hat{k}$, the principal axes of the confining potential, and their associated trapping frequencies, $\omega_i$, $\omega_j$, $\omega_k$. We characterize the residual asphericity, $(\omega_{\max}-\omega_{\min})/\bar{\omega}$, where $\omega_{\max}$, $\omega_{\min}$ and $\bar{\omega}$ are respectively the maximum, minimum and mean of $\omega_i$, $\omega_j$, $\omega_k$. The residual asphericity drifts with time, so we periodically retune and recharacterize the trap to keep asphericity small (typically less than 0.002). To minimize the undesirable mean-field potential, we work at temperature

[1]JILA, National Institute of Standards and Technology and University of Colorado, Boulder, Colorado 80309-0440, USA. [2]Department of Physics, University of Colorado, Boulder, Colorado 80309-0440, USA. *e-mail: lewandoh@colorado.edu

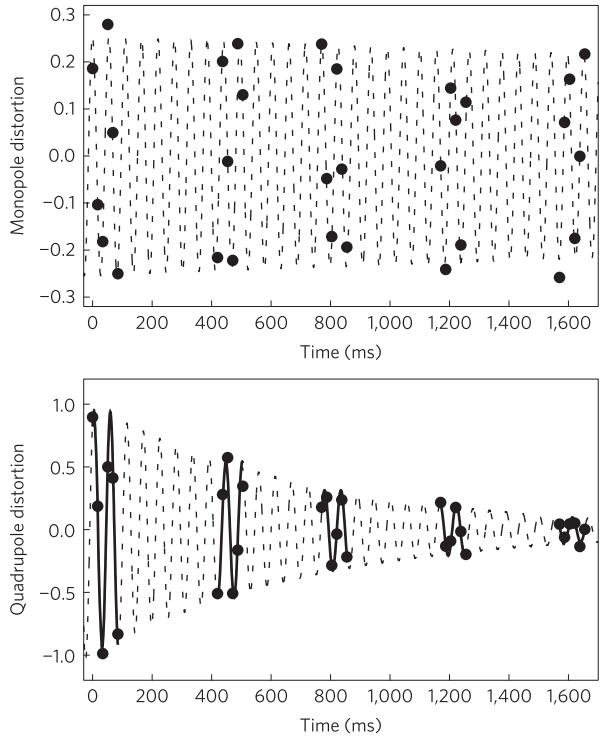


**Figure 1 | Sample data for a driven quadrupole mode and monopole mode in a spherical trap with residual asphericity less than 0.002 and a collision rate of 7.4(3) $s^{-1}$.** Solid lines on the quadrupole data indicate a typical fitting procedure, where individual periods taken in a single run are fitted with an undamped sine wave to extract an instantaneous amplitude. The oscillation amplitudes at various cycles are in turn fitted to an exponential decay to extract the damping rates shown in Fig. 2. Only a small subset of the monopole mode data is shown—the full set spans 30 s. Random observable scatter in these points is predominantly due to small, irreproducible fluctuations in initial conditions.

$T$ well above the Bose–Einstein condensate transition temperature, $T_c$, between $2T_c < T < 3T_c$.

We selectively drive monopole (quadrupole) motion by symmetrically (asymmetrically) modulating the strength of the confinement about its mean value. The cloud is then allowed to evolve freely in the spherical trap before it is non-destructively imaged using phase-contrast microscopy[13,14]. For each cycle of the experiment, six images are taken of the cloud along two orthogonal axes at an interval of 17 ms to sample roughly 1.5 oscillation periods. Cloud widths along each dimension, $\sigma_{i,j,k}$, are determined using Gaussian surface fits of individual images to determine the amplitude of the monopole and quadrupole modes. Amplitudes of the monopole and quadrupole distortion are scaled by the average width of the cloud during one cycle, given by the following relations

$$A_M = \frac{\sigma_i^2+\sigma_j^2+\sigma_k^2}{\langle\sigma_i^2+\sigma_j^2+\sigma_k^2\rangle} - 1$$

$$A_Q = \frac{2\sigma_k^2-\sigma_i^2-\sigma_j^2}{\langle\sigma_i^2+\sigma_j^2+\sigma_k^2\rangle}$$

Oscillation amplitudes are determined by fitting a cycle of oscillation in cloud width, obtained from each experimental run, with a fixed frequency sine wave as indicated by the solid lines in Fig. 1.

Suppressed damping of the monopole mode relative to the quadrupole mode can be seen in the sample data in Fig. 1, and although the monopole damping rate is small, it is non-zero. We characterize the monopole damping by comparing with quadrupole

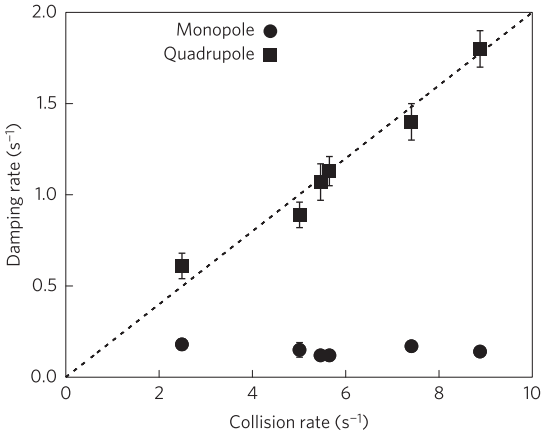


**Figure 2 | Monopole and quadrupole damping rates as a function of interatomic collision rate in a near-spherical trap.** The dotted line indicates the predicted quadrupole damping rates given in equation (4). Residual asphericity was typically around 0.001, but always less than 0.0026. Cloud full-width at half-maximum was approximately 115 μm. Error bars in the monopole data are smaller than the data points. There is a multiplicative uncertainty in the collision rate of 10%. Error bars are determined from exponential fits to the decay of instantaneous amplitudes.

mode damping rates, which are expected to vary linearly with collision rate. By adjusting the evaporation parameters in our experiment, we can tune $N$, $T$, and the collision rate of the sample, and then alternately drive quadrupole or monopole modes. A direct comparison of quadrupole and monopole damping rates in a near-spherical trap is shown in Fig. 2. The dependence of quadrupole damping on collision rate is $\Gamma_Q = 0.20(3)\ \gamma_{coll}$, which is in good agreement with equation (4). The small amount of residual damping in the monopole mode is independent of collision rate and much smaller than the damping in the quadrupole mode, as expected. This, then, is the special-case exception that proves the general rule of damping in the Boltzmann equation.

To understand the source of residual monopole damping, we note that Boltzmann's result hinges on the assumption that the potential is both isotropic and harmonic. An actual physical system can never satisfy both of these conditions perfectly, and the remainder of this letter is devoted to a discussion of the effects that small anisotropies and anharmonicities have on the monopole damping rate.

Certain subtleties arise for gases in the collisionless limit when anisotropies in the potential are small enough such that trap frequencies differ by less than a few percent. In a totally collisionless system, oscillations along the principal axes of the trap are fully decoupled and monopole- or quadrupole-like oscillations are undamped. If the principal trap frequencies differ such that $\omega_i = \omega_j \neq \omega_k$, dephasing occurs between oscillations along different principal axes and energy exchange between pure monopole motion and pure quadrupole motion occurs with a period given by

$$T_{MQ} = \frac{\pi}{|\omega_k - \omega_i|}$$

When collisions are included, the two modes become coupled and, as the population in the quadrupole mode increases, so does the damping[15]. This effect can be seen when $T_{MQ} < 1/\Gamma_Q$, where multiple oscillations between monopole and quadrupole modes occur. Data in Fig. 3 show oscillations between monopole and quadrupole modes resulting from an initial monopole drive in a trap with a residual asphericity of approximately 0.02. Energy transfers back and forth between the individual modes, and the damping rates for both modes are nearly equal, with a mean value of $\Gamma = 0.36(4)\ s^{-1}$. The collision rate is roughly 3.7 $s^{-1}$, leading to an expected quadrupole damping rate of 0.74 $s^{-1}$ in a spherical

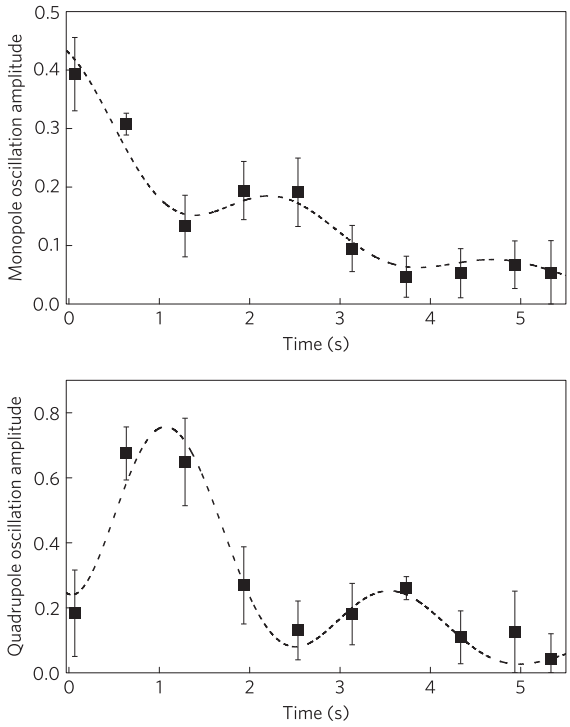


**Figure 3 | Monopole and quadrupole oscillation amplitudes in an anisotropic trap where the residual asphericity is approximately 0.02.** The data points show the amplitudes of individual oscillations of the instantaneous distortion, such as those indicated by the black lines in Fig. 1. A monopole mode is initially driven and oscillations between the monopole and quadrupole modes at a frequency $\Delta\omega$ can be seen. The dotted line fitting functions are $e^{-\Gamma t}(\cos^2(\Delta\omega t+\delta)+C)$ Amplitudes are determined from sine-wave fits to individual oscillation measurements obtained from a single experimental cycle. The error bars are calculated from scatter in the sine-wave fits of data taken at repeated evolution times.

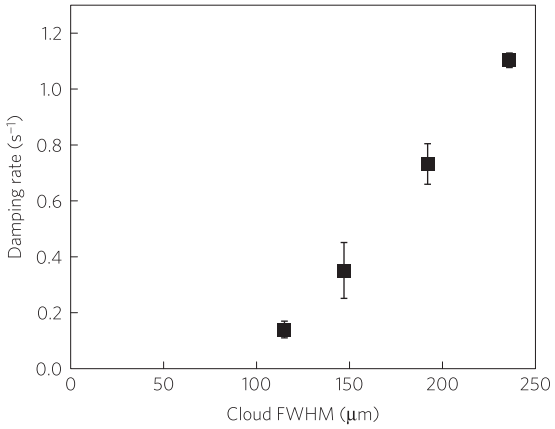


**Figure 4 | Damping of the monopole mode in a near-spherical trap as a function of the spatial extent of the atom cloud.** The fractional amplitude of the excitation is the same for all points. Consistent with anharmonicity-induced damping, we see the observed damping rate decreases rapidly for smaller clouds, but the trend of the data suggests that even for the smallest clouds (such as those used in Fig. 2) the residual damping observed may be due to the onset of anharmonic effects. The error bars are calculated using the same method as described in Fig. 3 and the error in the cloud width measurements were typically 5%.

trap, which is twice the value of the measured damping rate in the anisotropic trap. This is no surprise because the quadrupole mode is effectively populated only half of the time, leading to the factor of two decrease in the damping rate. If we decrease the amount of anisotropy such that $T_{MQ} \gg 1/\Gamma_Q$, the energy in the quadrupole mode damps before it can fully couple back into the monopole mode. One can see this effect in the data for the very spherical case shown in Fig. 1, where the quadrupole mode damps before it can exchange with the monopole mode. The data in Fig. 2 were taken in traps with residual asphericities ranging from 0.0005–0.0026, corresponding to $10.7\,\mathrm{s} < T_{MQ}/2 < 55.6\,\mathrm{s}$. Whether plotted versus collision rate, as shown, or versus $T_{MQ}$, we see no systematic trend in the residual monopole damping. Thus, some other physical effect must provide the dominant source of residual monopole damping.

We now come to the second condition of Boltzmann's result, which requires that the potential be harmonic, and discuss the effect of anharmonic perturbations to our trapping potential as a source of damping. Amplitude-dependent frequency shifts caused by anharmonic perturbations lead to dephasing of individual particle trajectories, effectively damping the collective monopole amplitude. Moreover, the anharmonic corrections to our potential are asymmetric, giving rise to an amplitude-dependent anisotropy. A calculation of the expected damping rate that takes into account all of the relevant anharmonic corrections is difficult. But the effect can be explored experimentally by measuring the monopole damping as a function of cloud size, as shown in Fig. 4. The first point in Fig. 4 represents the average of the cloud size and monopole damping data in Fig. 2. The trend of the data in Fig. 4 suggests that the residual damping seen even at the smallest cloud size of 115 μm is already due to the onset of anharmonic effects. Unfortunately, we are unable to work with smaller, and thus colder, clouds owing to limitations in the signal-to-noise ratio of our imaging system, and the need to keep $T \gtrsim 2T_c$.

In this paper, we present an experimental verification of the absence of damping for the monopole mode of a thermal gas in an isotropic harmonic potential. Whereas the damping is highly suppressed, the small, but finite, relaxation of the monopole mode is an artefact of small anharmonic perturbations to our trap, which decrease with cloud size. We find that, in the limit of zero anharmonic shifts, the damping of the monopole mode tends to zero, as predicted by Boltzmann in 1876 (ref. 1).

## Methods

Methods and any associated references are available in the online version of the paper.

Received 29 March 2015; accepted 25 August 2015; published online 5 October 2015

## References

1. Boltzmann, L. Über die Aufstellung und Integration der Gleichungen, welche die Molekularbewegung in Gasen bestimmen. *Sitz.ber., Akad. Wiss. Wien* **74,** 503–552 (1876).
2. Kinoshita, T., Wenger, T. & Weiss, D. S. A quantum Newton's cradle. *Nature* **440,** 900–903 (2006).
3. Chevy, F., Bretin, V., Rosenbusch, P., Madison, K. & Dalibard, J. Transverse breathing mode of an elongated Bose–Einstein condensate. *Phys. Rev. Lett.* **88,** 250402 (2002).
4. Lobser, D. S. *Observation of a Persistent Non-Equilibrium State in an Extremely Isotropic Harmonic Potential* PhD thesis (Univ. Colorado, 2015).
5. Huang, K. *Statistical Mechanics* (Wiley, 1987).
6. Pottier, N. *Nonequilibrium Statistical Physics: Linear Irreversible Processes* (Oxford Univ. Press, 2010).
7. Uhlenbeck, G. E. & Ford, G. W. *Lectures in Statistical Mechanics* (American Mathematical Society, 1963).
8. Cercignani, C. *The Boltzmann Equation and its Applications* (Springer, 1988).
9. Guery-Odelin, D., Zambelli, F., Dalibard, J. & Stringari, S. Collective oscillations of a classical gas confined in harmonic traps. *Phys. Rev. A* **60,** 4851–4856 (1999).
10. Pitaevskii, L. P. *Bose–Einstein Condensation* (Clarendon Press, 2003).
11. Petrich, W., Anderson, M. H., Ensher, J. R. & Cornell, E. A. Stable, tightly confining magnetic trap for evaporative cooling of neutral atoms. *Phys. Rev. Lett.* **74,** 3352–3355 (1995).

12. Ensher, J. R. *The First Experiments with Bose–Einstein Condensation of $^{87}Rb$* PhD thesis (Univ. Colorado, 1998).
13. Haljan, P. C. *Vortices in a Bose–Einstein Condensate* PhD thesis (Univ. Colorado, 2003).
14. Matthews, M. R. *Two-Component Bose–Einstein Condensation* PhD thesis (Univ. Colorado, 1999).
15. Buggle, Ch., Pedri, P., von Klitzing, W. & Walraven, J. Shape oscillations in nondegenerate Bose gases: Transition from the collisionless to the hydrodynamic regime. *Phys. Rev. A* **72,** 043610 (2005).

## Acknowledgements

This research was supported by the Marsico Fund and NSF grant PHY-1125844.

## Author contributions

D.S.L., A.E.S.B., E.A.C. and H.J.L. are jointly responsible for design of the experiment, analysis of data, and preparation of the manuscript. D.S.L. and A.E.S.B., in addition, collected the data.

## Additional information

Supplementary information is available in the online version of the paper. Reprints and permissions information is available online at www.nature.com/reprints. Correspondence and requests for materials should be addressed to H.J.L.

## Competing financial interests

The authors declare no competing financial interests.

## Methods

The undamped nature of the monopole mode is found by calculating the evolution of the squared radius of the cloud and can be derived in various ways[9]. It is instructive to see how the monopole non-damping result can be built up starting from $N=1$, 2, etc .... In spherical symmetry, the radial motion of a single particle of mass $m$, energy $E$, and angular momentum $L$ is governed by the effective potential[16]

$$V_e = \frac{L^2}{2mr^2} + \frac{1}{2}m\omega^2 r^2$$

so that the radial force is

$$m\frac{d^2r}{dt^2} = -\frac{d}{dr}V_e \tag{5}$$

and the kinetic energy is

$$\frac{1}{2}m\left(\frac{dr}{dt}\right)^2 = E - V_e \tag{6}$$

We note that $d^2r^2/dt^2 = 2(dr/dt)^2 + 2rd^2r/dt^2$, and substituting (5) and (6) yields the differential equation for $r^2$

$$\frac{d^2}{dt^2}r^2 = -\Omega^2(r^2 - r_0^2) \tag{7}$$

where $\Omega \equiv 2\omega$ and $r_0^2 = E/(m\omega^2)$. So the squared radius undergoes sinusoidal oscillations, or 'monopole breathe', around its mean value $r_0^2$ at a frequency of $2\omega$. If there are two particles, 1 and 2, each with individual values of $E$, $L$ and $r^2$, each particle will oscillate at $2\omega$. Taking the sum of their respective differential equations (7) yields

$$\frac{d^2}{dt^2}r_t^2 = -\Omega^2(r_t^2 - r_{0t}^2) \tag{8}$$

where their combined squared radius, $r_t^2 \equiv r_1^2 + r_2^2$, oscillates around its mean value, $r_{0t}^2 \equiv (E_1 + E_2)/(m\omega^2)$. The magnitude of the collective breathe motion depends on the magnitude and relative phase of the individual particle trajectories. These individual quantities will change abruptly in the event of a collision. Assuming the collisions are local, $r_1$, $r_2$, and thus $r_t^2$ will not change from the instant before to the instant after the collision. Similarly, momentum and energy conservation imply that $(d/dt)r_t^2$ and $r_{0t}^2$ are unchanged by the collision.

These three continuities imply that the parameters and boundary conditions of equation (8) are matched directly before and after a collision. This ensures that neither the magnitude nor phase of the oscillation will change as the result of a pairwise collision. If we instead consider $N$ atoms where

$$r_t^2 = \sum_{i=1}^{N} r_i^2$$

$$r_{0t}^2 = \frac{1}{m\omega^2}\sum_{i=1}^{N} E_i$$

one can see that the monopole mode is left unperturbed—and in particular undamped—by local, pairwise, momentum-, energy- and number-conserving collisions. This argument is robust to quantum statistics—Bose or Fermi—and, interestingly, in ref. 17, it is shown that a $1/r^2$ term in the potential also preserves monopole motion.

The above approach is consistent with a system in the hydrodynamic limit, with total number of atoms so large that the function $f(\mathbf{r},\mathbf{v},t)$ is essentially continuous. However, in the hydrodynamic limit, mean-field effects can come into play, in which case the monopole frequency is shifted[18]. In our experiment, the total number of atoms, $N$, is only a few hundred thousand, and the mean-free path is large compared to the spatial extent of the sample—we are not in the hydrodynamic limit in any sense of the word—and mean-field effects can be neglected.

## References

16. Thornton, S. *Classical Dynamics of Particles and Systems* (Brooks/Cole, 2004).
17. Guéry-Odelin, D., Muga, J. G., Ruiz-Montero, M. J. & Trizac, E. Nonequilibrium solutions of the Boltzmann equation under the action of an external force. *Phys. Rev. Lett.* **112,** 180602 (2014).
18. Guéry-Odelin, D. Mean-field effects in a trapped gas. *Phys. Rev. A* **66,** 033613 (2002).